A High Frequency Battery Model for Current Ripple Analysis

Jin Wang* Ke Zou
Department of Electrical and Computer Engineering
The Ohio State University
Columbus, OH, USA
*Wang@ece.osu.edu

Chingchi Chen* Lihua Chen
Ford Motor Company
Dearborn, MI, USA
*Cchen4@ford.com

Abstract—**In applications where batteries work together with power electronic circuits, the current ripple generated by the power electronics will be shared by both the battery and passive components in the circuit. The amount of ripple absorbed by the battery depends on its impedance at the switching frequency of power electronics. This paper presents an impedance based high frequency battery model derived from test results of a Ni-MH battery using a novel battery impedance tester. The possible reasons for the battery impedance characteristics in high frequency region, including skin effect and proximity effect, are also discussed. This battery model can be directly used in current ripple analysis, passive components design and control strategy optimization of power electronic circuits. The effect of the passive component values on the battery current ripple is analyzed using the ac equivalent circuit of the test setup.**

I. INTRODUCTION

In hybrid electric vehicles (HEV) and other applications, batteries usually work together with power electronics circuits such as dc/dc converters and dc/ac inverters, which generate significant amount of switching frequency related current ripple. The current ripple absorbed by the battery is determined by the impedance of the battery itself as well as other passive components such as its paralleled capacitor. Since the battery impedance changes with its operation frequency and current [1], the knowledge of the battery impedance at switching related frequencies and high current ripple conditions is the key in designing the passive components and optimizing the control strategy of the power electronic circuits.

Most battery impedance testing methods available today use small signal testers, such as the electrochemical impedance spectroscopy (EIS) [2], [3]. This may not be the best approach for power electronics related applications where high amplitude dc and ac are both present. This paper employs a novel impedance tester which uses a dc/dc converter to create a dc offset and ac ripple to produce an environment that mimics the operation of real power electronics.

For the battery modeling, equivalent circuit based battery models have been extensively studied [4], [5]. However, most of them are not suitable for power electronics circuit analysis since they are derived from test frequencies lower than 5 kHz and ac current ripples whose amplitude is much less than 5 A. The battery model developed in this paper focuses on the normal switching frequency range (5 kHz ~ 20 kHz) of power electronics in HEV operations and is developed from high AC current ripple tests (larger than 10 A peak to peak).

In section IV, the model is briefly analyzed. Possible reasons for the battery impedance behavior in switching frequency regions, including skin effect and proximity effect are investigated in the analysis. The effect of stray inductance in the accuracy of the model is also discussed.

Based on this model, the battery current ripple is analyzed using the ac equivalent circuit method with different passive component values. This analysis will help the passive components design and system stability analysis of power electronics circuits.

II. TEST SETUP AND TEST METHOD

The test setup diagram is shown in Fig. 1, which consists of a boost dc/dc converter, a high-accuracy film capacitor and the battery under test. In this test setup, the boost converters are realized using an integrated power module (IPM) rated at 1200V/200A. It is controlled by a TI TMS320F2812 DSP and functions as an ac ripple generator to produce triangular ripple on the inductor.

The high accuracy film capacitor works as an impedance reference. Under the assumption that the capacitance does not change with frequency, the impedance of the battery can be calculated from the current sharing relationship between the battery current and capacitor current. The capacitor current and battery current are measured according to the direction notation in Fig.1. Then the battery impedance Z can be calculated using (1),

$$|Z| = \frac{|i_c|}{|i_b|} \times \frac{1}{2\pi f C}, \angle Z = \angle i_c - \angle i_b + 90^\circ \quad (1)$$

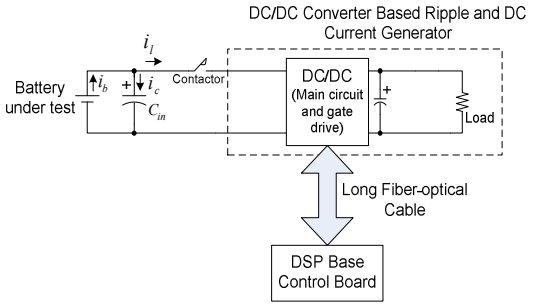

Figure 1. The general diagram of test setup.

where i_c , i_b are the switching frequency components of capacitor current and battery current, f is the switching frequency and C is the capacitance of the capacitor.

Experiments were conducted within a switching frequency range of 5 kHz to 20 kHz. A 6.5V Ni-MH battery from a current mass production hybrid vehicle was discharged to a resistive load through the boost converter. In the experiments, the battery is charged to 50% SOC and the discharging time for each test is limited to less than 3 seconds to ensure that in the whole experiment the SOC variation is less than 3%. The connection cable between the battery and the capacitor is intentionally twisted to reduce its stray inductance.

Fig.2 shows the test setup on the battery side. Fig. 3 shows the current test result under the condition of 10 kHz switching frequency and 100A dc offset. The battery current is almost in phase with the capacitor current. According to the notation of Fig. 1, this implies the battery impedance is inductive. Fig. 4 shows the battery impedance amplitudes and angles at different frequencies and 5A dc offset. The detailed test results can be found in [6].

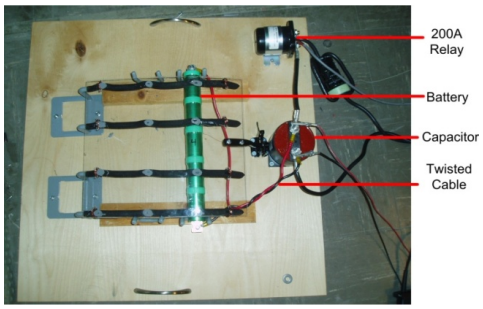

Figure 2. The test setup on the battery side.

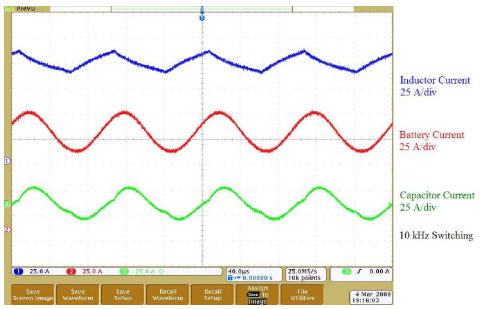

Figure 3. Current waveforms at 10 kHz, 100 A dc offset.

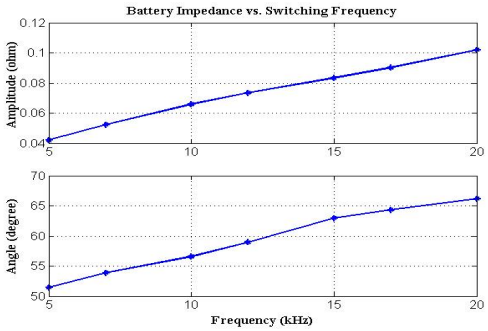

Figure 4. Impedance vs. switching frequency at 5A dc offset.

Current measurements were made with Tektronix TCP0150 current probes which have a typical dc error less than 1%. The measured current signal was recorded by a Tektronix 4054 digital oscilloscope operating in high resolution (Hi-res) mode. The digitizer of the oscilloscope is 11 bit at this mode. In the measurement the waveforms are adjusted to posses at least 4 vertical divisions (one half of the screen) so the digitization error is less than 0.1%. The recorded current data contains at least 1500 points per cycle which is processed by the computer using DFT to find out the switching frequency component. The overall measurement error could be controlled to be less than 3%. Since this system employs a current measurement method, it can test a battery cell or a string of batteries with the same level of accuracy. Other types of batteries and other energy storage devices such as fuel cells could also be tested using this tester.

III. Derivation of High Frequency, High Current Battery Model

The impedance based battery model can be derived using an approximation of the frequency response curve shown in Fig. 5 and Fig. 6. This paper employs an advanced vector fitting method introduced by Gustavsen [7]-[9]. This method approximates a frequency response f(s) with a rational function, expressed in the form of a sum of partial fractions:

$$f(s) \approx \sum_{m=1}^{N} \frac{c_m}{s - a_m} + d + se \qquad (2)$$

where terms d and e are optional. c_m and a_m are the residuals and poles, respectively.

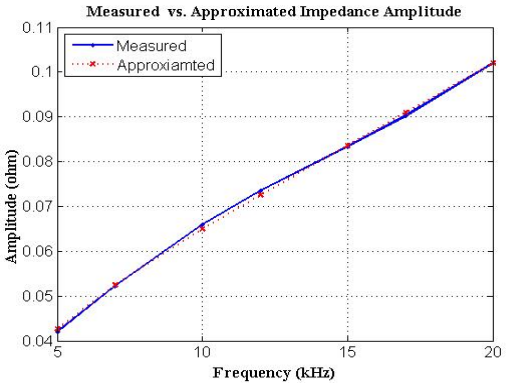

Figure 5. Measured and approximated impedance amplitude.

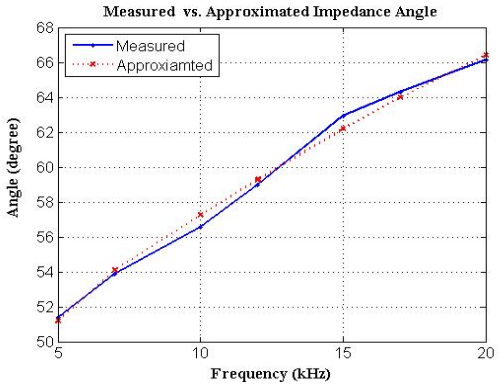

Figure 6. Measured and approximated impedance angle.

As shown in Fig. 6, in the frequency range from 5 kHz to 20 kHz, the battery impedance is inductive so d and e could not be omitted. Since the frequency response (both amplitude and angle) is quite linear, this implies one pole is enough to describe the battery impedance characteristic at this frequency range, so m=1. Using the vector fitting code provided by Gustavsen [10] and the above restrictions, parameters in (2) are found to be:

$d = 0.0437, e = 6.8014\times10^{-7}, a_1 = -4.484\times10^{4}, c_1 = -1131.5.$

Then the battery current-voltage transfer function can be written as (3).

$$Z_{batt}(s) \approx \frac{-1131.5}{s+44842} + 0.0437 + 6.801\times10^{-7}s \qquad (3)$$

The approximated and measured curve of battery impedance amplitude and angle are compared in Fig. 5 and Fig. 6, respectively. Since (3) is a second order transfer function, the impedance based battery model is proposed as shown in Fig. 7, which consists of two inductors and two resistors. From Fig.7, the battery impedance can be expressed as (4):

$$Z_{batt}(s) = L_1 s + R_1 + \frac{L_2 R_2 s}{L_2 s + R_2} = \frac{L_1 L_2 s^2 + (L_1 R_2 + L_2 R_1)s + R_1 R_2}{L_2 s + R_2} \qquad (4)$$

Comparing (3) and (4), each component in Fig. 7 can be calculated as shown in Table I.

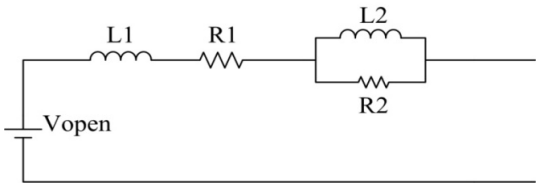

Figure 7. The proposed high frequency battery model.

TABLE I. PASSIVE COMPONENTS PARAMETERS IN THE PROPSED BATTERY MODEL

Component	Value
L1	0.680 μH
R1	0.0184 Ω
L2	0.562 μH
R2	0.0252 Ω

IV. MODEL ANALYSIS

The model presented in Fig.7 is a simple one aiming to help with the design and control of power electronic circuits. The obvious differences of this model from normal low-frequency models are the addition of inductive components and the elimination of capacitive components. These reflect the battery's inductive behavior at normal switching frequency range. The paralleled L-R branch represents the fact that the equivalent inductance decreases as the frequency increases. It should be noted that extra capacitive components, such as the traditional R-C branches, can be added in the model to make it more accurate. However, this model makes the process easier for ripple analysis and power electronics design.

The battery's inductive behavior at high frequency is due to its intrinsic inductance which is usually been neglected in the low frequency region. Previous studies on battery's impedance at high frequency also include inductive components in the model. For example, in [1], an inductor is added to the circuit model. However, those works were not focused on the power electronics switching frequency so the frequency range is usually from 0.01 Hz to several kHz and the ac ripple is much less than 10 A. So their results either did not cover the switching frequency region, or had different impedance response, in both amplitude as well as phase, from the one described in this paper.

The stray inductance of the connection cables between the battery and the capacitor also contributes to part of the total inductance in the model. The amount of stray inductance is decided by the cable-battery loop area and the width of the cables. Using twisted cable or specially designed busbar could eliminate most of the stray inductance. For example, if the cables in Fig. 2 are not twisted together, the stray inductance could be as large as several hundreds of nanohenry. However, if they are twisted together, the stray inductance could be reduced to several tens of nanohenry which will significantly increase the accuracy of the battery impedance measurement in the test.

The test results also show that, together with the decrease or equivalent inductance, the battery resistance actually increases with the frequency. These facts provide us clues as to the possible reasons for this battery impedance characteristic in switching frequency region:

A. Skin Effect

Skin effect is the unequal distribution of ac current within a conductor. The surface of the conductor tends to have more current density than in the middle. This leads to an increase of resistance and decrease of inductance of the conductor in ac conditions compared to dc. For the battery, since its diameter is much larger than the skin depth, the resistance is approximately proportional to the square root of switching frequency.

A frequency sweeping test is performed to find out the possible relationship between the skin effect and battery impedance characteristic at switching frequency region. In this test, the battery is place far from any conductors and the test frequency ranges from 4 kHz to 20 kHz with a step of 1 kHz. The battery resistance is calculated and normalized with

respect to the resistance at 4 kHz, i.e. if the resistance at 4 kHz is r_0, the normalized resistance r_n for a measured resistance r is $r_n = r / r_0$. The square root of switching frequency is also normalized with respect to the square root of 4000 Hz and plotted together with the normalized resistance in Fig.8.

It can be seen in Fig.8 that the change of resistance of the battery in the tested frequency region generally follows the square root of switching frequency. This indicates that the skin effect could be a possible source for the high frequency behavior of battery.

B. Proximity Effect

The proximity effect accounts for the fact that the current distribution within one ac-carrying conductor is affected by other conductors close to it. The proximity effect will also increase the equivalent resistance of the conductor. A frequency sweeping test is performed in which the battery is bounded together with a cable that is carrying same amount of current as the battery but in the opposite direction. Fig. 9 shows the test results. It can be seen that at lower frequencies (less than 15 kHz), the resistance follows the curve of square root of frequency. Then at the region above 15 kHz, the resistance soars, which possibly implies the influence of the proximity effect.

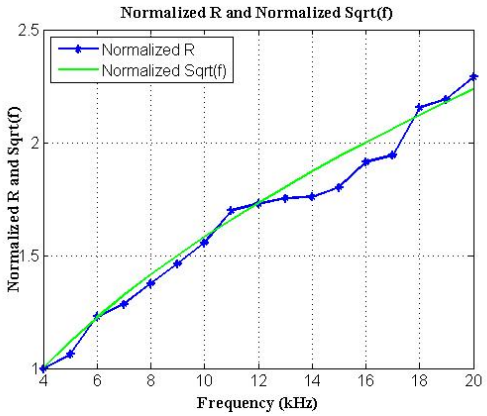

Figure 8. The normalized R and normalized square root of switching frequency without nearby conductors.

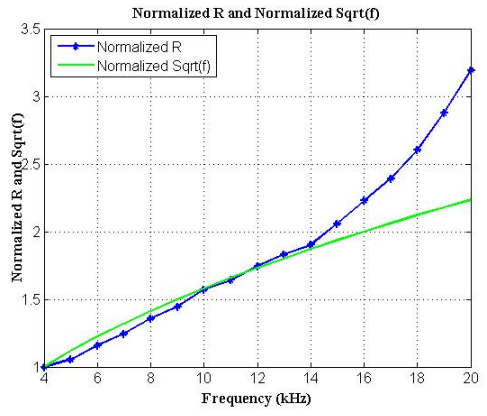

Figure 9. The normalized R and normalized square root of switching frequency with nearby conductors.

The proximity effect increases the inaccuracy of battery impedance testing. So in the tests, the battery should be placed away from other conductors to reduce their influence.

V. AC EQUVALENT CIRCUIT ANALYSIS

The purpose of the derived battery model is to help with battery ripple analysis. In [11], an ac small signal circuit is introduced to analyze the voltage ripple on photovoltaic cells. Similarly, here the ac equivalent circuit of the test setup is used to analyze the ac ripple on the battery. For the battery discharge mode, the boost converter is replaced by a square voltage source V_{sq} operating at switching frequency to generate ac ripple, as shown in Fig. 10 (a).

The boost converter inductor L, the capacitor C and equivalent battery inductance work together as a LCL filter. So the square wave voltage source V_{sq} can be replaced by its fundamental V_1, as shown in Fig. 10(b). The amplitude of V_1 can be calculated using (5):

$$V_1 = \frac{2}{\pi}\sin((1-D)\pi)V_{out} \tag{5}$$

where V_{out} is the amplitude of boost converter output voltage.

This replacement will cause error since V_1 does not include battery current harmonics, which depends on the duty ratio D. For cases with large THD, V_{sq} could be simulated by several sinusoidal sources including V_1 and low order harmonics. In real HEV applications, a 285V battery, consisting of a string of 44 batteries, is used. So all of the parameters in Table I are multiplied by 44 in the simulation. For the component values specified here, the THD of I_{batt} is 0.8% when D=0.5 and is 12.6% when D=0.2.

The impedances of C, L and the whole circuit are $Z_c(s) = \frac{1}{Cs}, Z_L(s) = Ls, Z_{total}(s) = Z_L(s) + Z_c(s) // Z_{batt}(s),$ respectively. Thus, the amplitude of battery current ripple can be expressed as (6):

$$I_{batt} = \left| \frac{V_1}{Z_{total}(s)} \cdot \frac{Z_C(s)}{Z_{batt}(s) + Z_C(s)} \right| \tag{6}$$

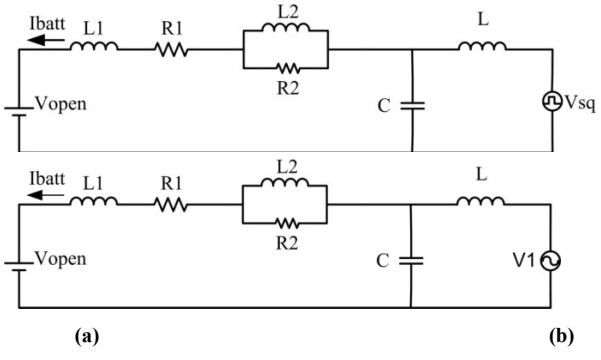

Figure 10. The ac equivalent circuit (a) square waveform source (b) sinusoidal waveform source.

Fig. 11 shows the battery current ripple magnitude as a function of L and C at a switching frequency of 10 kHz and 0.5 duty ratio. This result gives a direct indication on C and L selection. For example, if the maximum battery current ripple allowed is 0.5 A, the C could be selected as 260 μF and L is 260 μH . To verify the current ripple calculated here, PSIM was used to simulate the circuit in Fig.10 (a) under the following condition: C=260 μF and L=260 μH . The simulation result is shown in Fig. 12 and the current ripple amplitude is about 0.49A, which is consistent with the result of the previous calculation.

VI. CONCLUSIONS

This paper presents a high frequency, high current battery model based on the test results on a Ni-MH battery. This model only consists of two resistors and two inductors so it can be easily used in battery ripple analysis and the control strategy design for power electronics systems. The possible reasons for the battery impedance under high frequency, high ac current conditions, including the skin effect and the proximity effect are also investigated. Using the ac equivalent circuit of the battery impedance test apparatus, the influence of passive component values on battery current ripples is studied.

This paper is the first in a series of papers to investigate the impedance based battery model for high current and high frequency conditions. Fig. 13 shows the main circuit of the automatic tester which will be built in the next step. A grid-tied H-bridge inverter is added into the automatic tester. In this scheme, during the battery discharge mode, the battery works as a dc source by providing power to the utility grid and during the charge mode it absorbs power from the utility grid. A dSPACE controller is employed to control the battery current and realizing SOC tracking. Effort will also be made on detailed analysis of high frequency battery characteristics, power electronics system stability analysis and control strategy optimization.

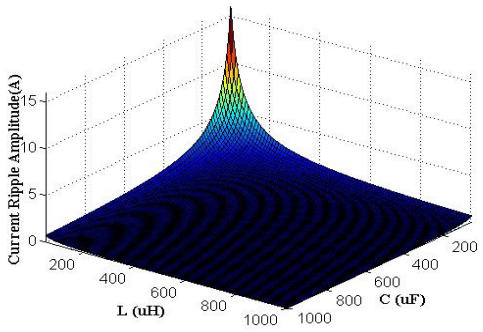

Figure 11. Battery current ripple vs. C and L.

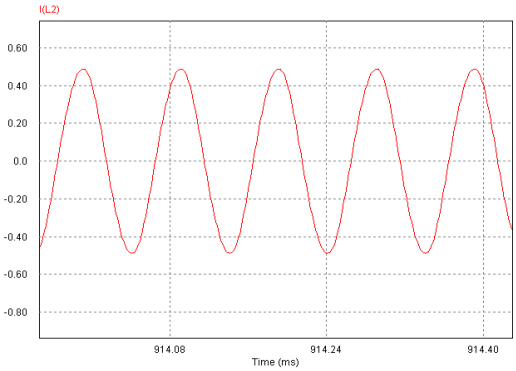

Figure 12. Simulated battery current ripple (C=260 μF , L=260 μH).

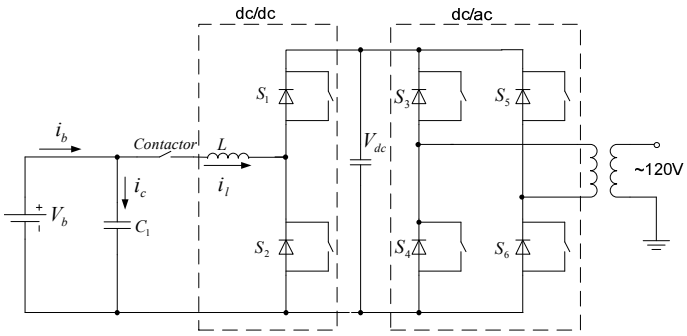

Figure 13. The main circuit for the automatic battery tester.

REFERENCES

[1] S. Buller, M, Doncker and E. Karden, "Impedance-based simulation models of supercapacitors and Li-Ion batteries for power electronic applications," IEEE Trans. Industry Applications, vol. 41, no. 3, MAY/JUNE 2005, pp. 742-747.

[2] P. Mauracher and E. Karden, "Dynamic modelling of lead/acid batteries using impedance spectroscopy for parameter identification," J. Power Sources, vol.67, Aug. 1997,pp. 69-84.

[3] X.Feng and Z. Sun, "A battery model including hysteresis for State-of-Charge estimation in Ni-MH battery," in IEEE 2008 Vehicle Power and Propulsion Conference,Sept. 2008, pp. 1–5.

[4] M.Chen, G.Rincon-Mora, "Accurate Electrical Battery Model Capable of Predicting Runtime and I–V Performance," IEEE Trans. Energy Conversion, vol.21, no.2, June 2006, pp.504-511.

[5] R. Kroeze and P. Krein, "Electrical Battery Model for Use in Dynamic Electric Vehicle Simulations," in IEEE 2008 Power Electronics Specialists Conference, June 2008, pp.1336-1342.

[6] Stephen Nawrocki, Renxiang Wang, Ke Zou and Jin Wang ,"High Current Battery Impedance Testing for Power Electronics Circuit Design Optimization," in IEEE 2009 Vehicle Power and Propulsion Conference, Sept. 2009.

[7] B. Gustavsen and A. Semlyen, "Rational approximation of frequency domain responses by Vector Fitting," IEEE Trans. Power Delivery, vol. 14, no. 3, pp. 1052-1061, July 1999.

[8] B.Gustavsen, "Improving the pole relocating properties of vector fitting," IEEE Trans. Power Delivery, vol. 21, no. 3, pp. 1587-1592, July 2006.

[9] D. Deschrijver, M. Mrozowski, T. Dhaene, and D. De Zutter, "Macromodeling of multiport systems using a fast implementation of the vector fitting method," IEEE Microwave and Wireless Components Letters, vol. 18, no. 6, pp. 383-385,June 2008.

[10] B. Gustavsen, User's guide for vectfit3.m. SINTEF Energy Research, N-7465 Trondheim, Norway. [Online]. Available: http://www.energy.sintef.no/Produkt/VECTFIT/index.asp : VFIT3.zip

[11] N.Benavides. P. Chapman, "Modeling the effect of voltage ripple on the power output of photovoltaic modules," IEEE Trans. Industrial Electronics, vol 55, Issue 7,July 2008 pp. 2638-2643.